

# Process Capability Optimization of Thermoplastic Polyurethane (TPU) Printed Parts in Fused Deposition Modeling Process

Rupesh Chalisgaonkar<sup>1\*</sup>, Deepak Kumar Yaduvanshi<sup>2</sup>, Shyam Kumar Birla<sup>3</sup>, Pardeep Kumar<sup>4</sup>, Vipin Kumar Sharma<sup>5</sup>

## Abstract

*Fused Deposition Modelling (FDM) 3D printing process requires precise printed dimensions with a special assessment of process parameters using Taguchi optimization methodology. The proposed research aims to determine the optimal parametric setting to maximize the process capability index of diametral deviation and roundness of product in 3D printing process of TPU (thermoplastic polyurethane). The input factors for printing TPU in this research include the extrusion temperature, cooling fan speed, infill density, and infill pattern. The geometric fidelity of TPU printed parts must be maintained due to its viscoelastic nature. The parametric optimization should be performed for printing dimensionally stable parts. The L9 Taguchi orthogonal array was used as a set of experiments for selecting the best parametric setting using signal-to-noise (S/N) ratio. The outcome of this investigation shed light on how the infill pattern and infill density affect the printed specimen's roundness and dimensional deviation, respectively. As the TPU is majorly used in aerospace industries, automotive industries, medical industries, and toy industries, the proposed work will provide benefit to achieve the accurate printed parts used to make the product. The outcome of this study could be useful to enhance sustainability in manufacturing by decreasing part rejections and subsequently energy saving and reducing the material wastage.*

**Keywords:** TPU (thermoplastic polyurethane), Fused deposition modeling, Process Capability Index, Taguchi, Roundness, Diametral deviation

### \*Author for Correspondence

Rupesh Chalisgaonkar

<sup>1</sup>Associate Professor, Department of Mechanical Engineering, MEDICAPS University, Indore, Madhya Pradesh, India

<sup>2</sup>Assistant Professor, Department of Mechanical Engineering, MEDICAPS University, Indore, Madhya Pradesh, India

<sup>3</sup>Assistant Professor, Department of Mechanical Engineering, MEDICAPS University, Indore, Madhya Pradesh, India

<sup>4</sup>Assistant Professor, Department of Mechanical Engineering, Maharishi Markandeshwar (Deemed to be University), Ambala, Haryana, India

<sup>5</sup>Professor, Department of Mechanical Engineering, Meerut Institute of Engineering and Technology, Meerut, Uttar Pradesh, India

Received Date: 05 September 2025

Accepted Date: 24 October 2025

Published Date: 21 March 2026

**Citation** Rupesh Chalisgaonkar, Deepak Kumar Yaduvanshi, Shyam Kumar Birla, Pardeep Kumar, Vipin Kumar Sharma. Process Capability Optimization of Thermoplastic Polyurethane (TPU) Printed Parts in Fused Deposition Modeling Process. Journal of Polymer & Composites. 2026; 14(Special Issue 1): S1846–S1864p.

## INTRODUCTION

In recent years, fused deposition modeling, or FDM, has become increasingly popular as a 3D printing process. It works by heating a spool of thermoplastic filament to a temperature less than its melting temperature and then extruding the heated filament through a nozzle to create a three-dimensional object in alternate layered structure. FDM is known for its versatility, speed, and low cost compared to other 3D printing technologies. The schematic diagram of the manufacturing process is shown in Figure 1. It consists of cylindrical filaments, usually 1.75 mm or 2.85 mm in diameter, which is first fed into the extrusion head. The thermoplastic material is heated and extruded by the extrusion head via a tiny nozzle, typically with a diameter of around 0.50 mm. The extruding material exiting from nozzle follows the path generated by

slicing software. The material gets deposited in a manner of alternate layer structure till the final component is made as per the design.

FDM can produce parts that have intricate profile which need no further assembly process, resulting in lowering the cost of production. It eliminates making the die and mold alteration due to frequent changes of its design as customized products could be made without making die and mold. Previous research shows that layer thickness, layer width and air gap are the main influential process parameters affecting the quality of the printed parts. Thermoplastic characteristics of polymer filament makes joining of layers easily at room temperature in FDM process [1, 2]. This process is having low cost, highly customized process but having limitation in terms of poor surface finish and limited constraints of thermoplastic materials [3]. Most thermoplastic materials used are Acrylonitrile Butadiene Styrene (ABS), Polylactic Acid (PLA), Thermoplastic Polyurethane (TPU), Nylon and Polyether Ether Ketone (PEEK) [4-7]. TPU has higher amount of elasticity, abrasion resistance, toughness, and low melting temperature [8-11]. TPU is used to make flexible components such as gaskets, seals, and footwear prototypes in different industrial sectors such as automotive, aerospace, and consumer goods. TPU is also used to make robotic components. Prosthetics, orthotics, and patient-specific implants are also majorly made by TPU in biomedical industry [12-13]. TPU materials are also being used to make tyers due to higher amounts of elasticity and ease of processing. TPU materials can be recycled and reused in place of rubber which enables its major use to make non pneumatic tyers in automobile industries [14-17].

The subsequent post processing operations are required to make the parts industry ready. The Additive Manufacturing process and Injection Molding Process could be compared based on case-to-case basis to produce polymer parts [18-21]. It was found from previous research that part orientation plays a major role in influencing the dimensional accuracy of printed parts in FDM process. The past literature reveals the influence of different process variables on dimensional accuracy in FDM process [22-27]. The Taguchi-based grey relational analysis methodology was applied to optimize the FDM parameters for TPU used in automotive parts. The surface quality and mechanical properties were investigated to select the best parametric condition in FDM process [28]. ANFIS model was developed to predict and optimize FDM process parameters for TPU material. The tensile strength, flexibility, and surface quality were examined to optimize and predict the best parametric conditions in FDM process [29]. The laser based in situ measurement was investigated to correlate the surface finish with the mechanical properties of liquid crystal polymer in FDM process. The autonomous data-driven method was applied to optimize the FDM process parameters [30]. The design optimization framework was applied to simulate the deposited heating material to measure the objective function. Gradient-based and gradient-free optimization methods were developed to select the effectiveness and utility of these methods [31]. The effect of infill patterns (zigzag and gyroid) on the mechanical properties of Fused Deposition Modelling (FDM) 3D printing process was studied. The other input parameters such as nozzle temperature, print speed, and bed temperature were also considered in this study using TPU material [32]. The impact of FDM process parameters (infill percentage and layer thickness) were investigated on tribological behavior of ABS and PLA parts. Multi-response optimization methodology and analysis of variance (ANOVA) were applied to study the effect of input parameters on coefficient of friction, surface finish, and wear [33].

Although FDM is one of the most popular technologies among additive manufacturing processes for printing customized parts, it still have some limitations such as anisotropic behavior, dimensional accuracy and poor surface finish. Several studies have focused on improving the mechanical properties, surface finish and process optimization of polymer such as PLA, ABS and PEEK, However, very limited research has addressed the dimensional fidelity of TPU components, especially with respect to quantifying process capability using statistical indices.

TPU's viscoelastic and flexible nature makes it highly sensitive to process variations, which often leads to shape distortion and poor dimensional control. Prior studies have mainly explored mechanical

or tribological characteristics of TPU but none have systematically evaluated the process capability index (PCI) for dimensional accuracy metrics such as diametral deviation and roundness. Moreover, the influence of infill pattern and infill density which are the critical parameters for geometrical stability of TPU printed parts, has not been comprehensively analyzed. The proposed work fills a significant research gap by establishing a statistical framework to evaluate and enhance the dimensional accuracy of flexible TPU parts, which is vital for their reliable use in industrial and biomedical applications.

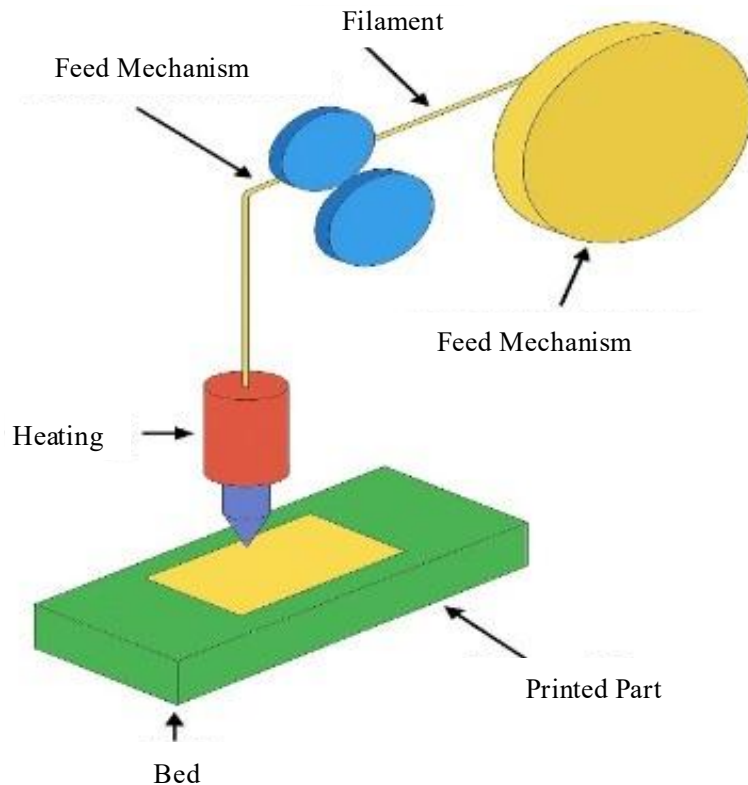


**Figure 1.** Schematic Diagram of Fused Deposition Modeling (FDM) 3D Printing Process

## MATERIALS AND METHODS

This study used Premium Thermoplastic Polyurethane (TPU)-95 as the filament material having 2.85 mm-diameter Jet-Black filament. The TPU specimens utilized in this investigation were manufactured using additive manufacturing technology (specifically an Ultimaker 2+ 3D printer) with Fused Deposition Modelling (FDM) capabilities. A reel of 2.85 mm diameter TPU filament was attached on a mounting spool that rests above the 3D printer. SolidWorks software was used for modelling the specimen. After that, the model was exported in the stereolithography (STL) file format allowing it to be read by the Cura program. This program slices the 3D model according to the chosen process settings. Subsequently, the sliced model is saved as a G-Code and produced using a 3D printer. The maximum building parts for this FDM printer is 223 mm x 220 mm x 205 mm (Figure 2). Selected process parameters with their level keeping other factors at constant level considered in this study are shown in Table 1. Figure 3 shows the infill patterns selected in this study to manufacture the specimen.

**Table 1:** Process Parameters with their Levels

Printing Parameter	Level 1	Level 2	Level 3
Extrusion Temperature (°C)	200	215	225
Cooling fan speed (%)	20	60	100
Infill Density (%)	20	60	100
Infill Pattern	Grid	Tri-Hexagonal	Triangular

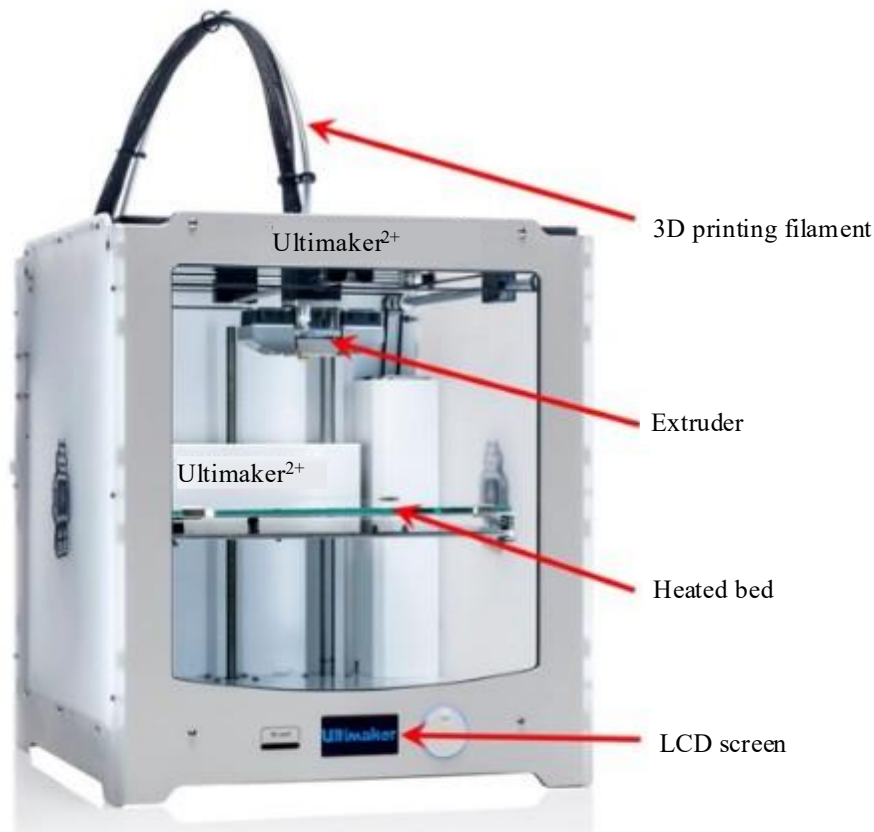


**Figure 2.** Ultimaker 2+ FDM 3D printer

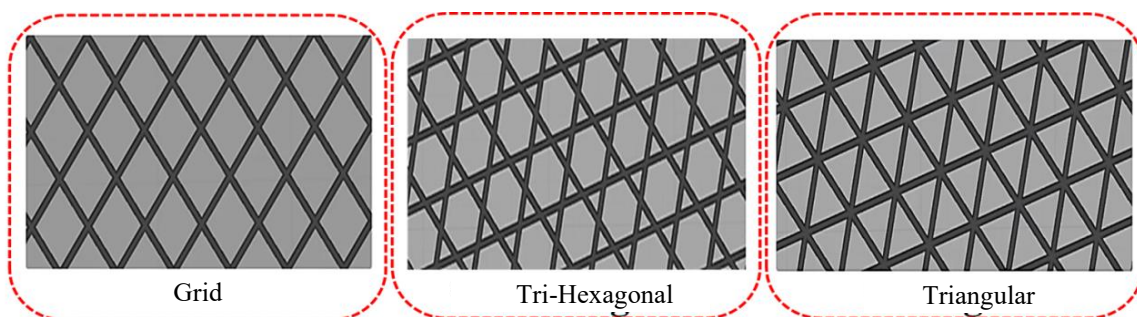


**Figure 3.** Infill Patterns to Print the FDM Specimens.

This work employs the Taguchi L-9 orthogonal array which enables the efficient optimization with fewer experiments compared to previous RSM or ANFIS based studies as discussed in literature review section. Process capability Index (PCI) analysis provides a quantitative measure of process robustness and effectiveness of the optimized parameters. The proposed novel approach highlights the practical advantages and advancement of the current study over earlier models. The Taguchi L9 orthogonal array was selected to efficiently evaluate the influence of key process parameters with a minimum number of experiments extrusion temperature, cooling fan speed, infill density and infill pattern (each at three level) with a 9 experiments (Table 2). This design focuses on the main effects, which are known to have the most significant influence on the dimensional analysis of printed parts, while higher order interaction effects are considered negligible in the present study.

One sample was printed after each experiment and measurement was carried out at three places for evaluating the average value of diametral deviation and roundness. All 9 prints were performed using the same filament batch and printer setting, and the run order was randomized to minimize the influence



**Table 2.** L-9 Orthogonal Array

Extrusion Temp.(C)	Cooling fan speed (%)	Infill Density (%)	Infill Pattern
200	20	20	Grid
200	60	60	Tri-Hexagonal
200	100	100	Triangular
215	20	60	Triangular
215	60	100	Grid
215	100	20	Tri-Hexagonal
225	20	100	Tri-Hexagonal
225	60	20	Triangular
225	100	60	Grid

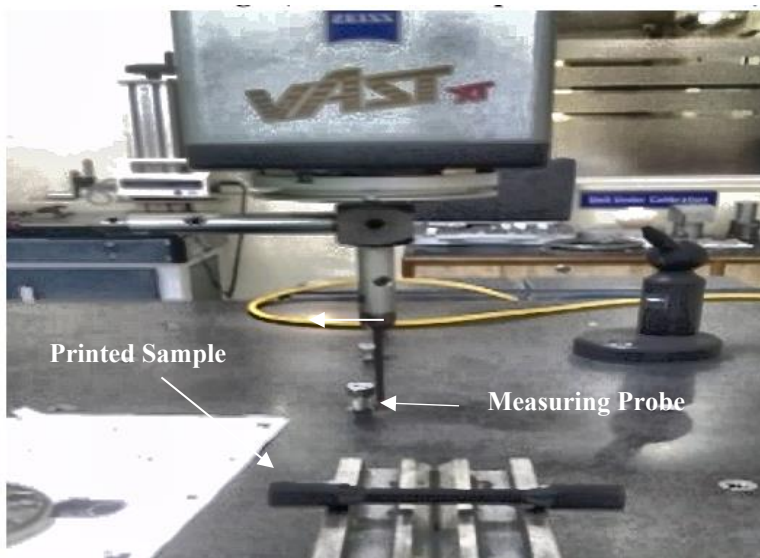
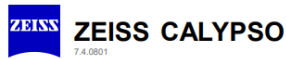


**Figure 7. (a)** Pictorial View of CMM ZEISS CALYPSO (Close View) used for Measurement the Specimen



**Figure 7. (b)** CMM ZEISS CALYPSO used for Measurement the Specimen



Part name **Measurement plan 54**

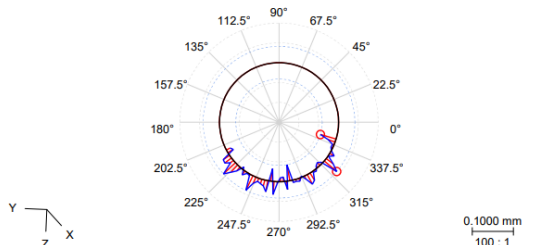
Drawing number  
 Order number  
 Variant  
 Company  
 Department  
 CMM Type  
 CMM No.  
 Operator  
 Text

CONT\_G2  
 194707  
 Master

Last 1 measurements  
 ► Approval ≠ Blocked  
 Part ident 3  
 Time/Date 4/24/2023 11:44 AM  
 Run All Characteristics  
 No. measured values 7  
 No. values: red 6  
 Measurement Duration 00:01:33.0

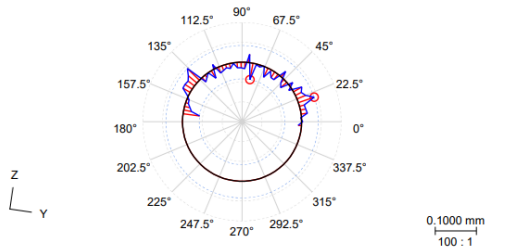
Name	Measured value	Nominal value	+Tol	-Tol	Deviation	+/-
DiameterCircle1	15.8901 mm	16.0000	0.2000	-0.2000	-0.1099	
DiameterCircle2	15.7265 mm	16.0000	0.2000	-0.2000	-0.2735	-0.0735
DiameterCircle3	9.4460 mm	10.0000	0.2000	-0.2000	-0.5540	-0.3540
Cartesian Distance1	119.2857 mm	120.0000	0.2000	-0.2000	-0.7143	-0.5143
Roundness1	0.0792 mm	0.0000	0.0000	0.0000	0.0792	0.0792

Points 46  
 Filter type No Filter  
 Lc  
 upr  
 Vmess[mm/sec] 9.50  
 Probe radius 1.5012  
 Evaluation method Minimum Feature

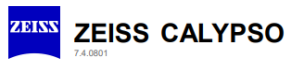


Roundness2	0.0810 mm	0.0000	0.0000	0.0000	0.0810	0.0810
------------	-----------	--------	--------	--------	--------	--------

Points 48  
 Filter type No Filter  
 Lc  
 upr  
 Vmess[mm/sec] 9.50  
 Probe radius 1.5012  
 Evaluation method Minimum Feature



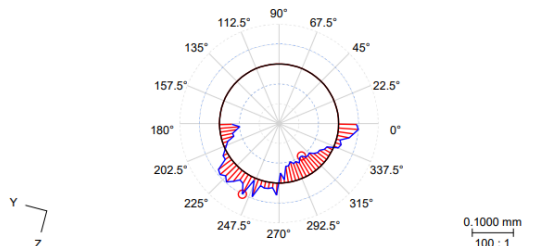
8.2\_001 Standard Protocol



Part name **Measurement plan 54**  
 Order number  
 Part ident 3  
 Operator Master  
 Time/Date 4/24/2023 11:44 AM

Name	Measured value	Nominal value	+Tol	-Tol	Deviation	+/-
Roundness3	0.0975 mm	0.0000	0.0000	0.0000	0.0975	0.0975

Points 50  
 Filter type No Filter  
 Lc  
 upr  
 Vmess[mm/sec] 1.00  
 Probe radius 1.5012  
 Evaluation method Minimum Feature



Text  Event

n.def.

Figure 8. CMM Report of Sample 1

## Evaluation of Process Capability Index

### Diametral Deviation

Process capability index of diametral deviation was evaluated by comparing the diameter of the specimen measured by ZEISS CALYPSO CMM with CAD image value.

$$\text{Diametral Deviation at each section (mm)} = \text{Measured Diameter (in mm)} - \text{Diameter (in mm) as per CAD image} \quad (1)$$

Mean value of Diametral Deviation in mm for each specimen ( $X_{\text{mean}}$ ):

It is calculated by following equation.

$$X_{\text{mean}} = \frac{\text{Diametral Deviation at section 1} + \text{Diametral Deviation at section 2} + \text{Diametral Deviation at section 3}}{3} \quad (2)$$

Standard deviation ( $\sigma$ ): Standard deviation for each specimen is calculated by the following equation.

$$\text{Standard deviation } (\sigma) = \sqrt{\frac{\sum_{i=1}^3 (x_i - X_{\text{mean}})^2}{3}} \quad (3)$$

Where  $x_i$  represents the value of each diametral deviation for each specimen.

Process capability index (PCI) for each specimen: Process capability index can be evaluated by the following equation.

$$\text{Process Capability index (PCI)} = \text{Min} \left\{ \frac{\bar{X} - \text{LSL}}{3\sigma}, \frac{\text{USL} - \bar{X}}{3\sigma} \right\} \quad (4)$$

Where

USL= Upper specification limit for each measuring characteristics (+0.5 mm)

LSL= Lower specification limit for each measuring characteristics (-0.5 mm)

The USL and LSL of  $\pm 0.5$  mm for PCI calculation were chosen based on typical dimensional tolerance for polymer FDM parts. These limits provide a practical range to compare the effect of process parameters on geometric accuracy.

Table 3 exhibits the computation of PCI of diametral deviation of all specimens with S/N ratio.

### Roundness

The roundness was measured at each section of the specimen and mean value is taken for evaluation of process capability index (PCI). The evaluation steps for PCI calculation of roundness are same as considered for diametral deviation. Table 4 exhibits the computation of PCI of roundness of all specimens with S/N ratio.

**Table 3.** Process Capability Index (PCI) of Diametral Deviation With S/N Ratio

S. No.	Deviation1	Deviation 2	Deviation 3	Mean ( $\bar{X}$ )	SD ( $\sigma$ )	PCI	S/N ratio
1	-0.1099	-0.2735	-0.554	-0.312	0.225	0.278	-11.1191
2	0.2178	0.1582	0.122	0.166	0.048	2.298	7.227
3	0.4872	0.2738	0.250	0.337	0.131	0.416	-7.61813
4	0.0794	0.0772	-0.077	0.027	0.090	1.761	4.915187
5	1.0722	0.5696	0.233	0.625	0.422	0.099	-20.0873
6	-0.0007	-0.0828	-0.230	-0.104	0.116	1.137	1.115209
7	0.5697	0.4787	0.364	0.471	0.103	0.094	-20.5374
8	0.1879	0.2334	-0.048	0.124	0.151	0.828	-1.63939
9	0.4872	-0.2778	-0.247	-0.012	0.433	0.375	-8.51937

**Table 4.** Process Capability Index (PCI) of Roundness With S/N Ratio

Exp. No.	Roundness 1	Roundness 2	Roundness 3	Mean ( $\bar{X}$ )	SD( $\sigma$ )	PCI	S/N ratio
1	0.079	0.081	0.098	0.086	0.010	2.839	9.0633
2	0.126	0.127	0.100	0.118	0.015	2.532	8.0693
3	0.140	0.139	0.091	0.124	0.028	1.479	3.3994
4	0.096	0.181	0.077	0.118	0.055	0.707	-3.0116
5	0.301	0.286	0.114	0.234	0.104	<b>3.211</b>	10.1328
6	0.080	0.081	0.074	0.079	0.004	6.648	16.4538
7	0.153	0.155	0.181	0.163	0.016	2.891	9.2210
8	0.174	0.219	0.241	0.211	0.035	0.853	-1.3810
9	0.072	0.067	0.083	0.074	0.008	2.930	9.3374

## RESULT AND DISCUSSION

### Diametral Deviation

In this research work diametral deviation was studied with roundness to map the inaccuracy of the printed specimen's dimensions. The main effects plots and signal-to-noise ratio were plotted using Taguchi's design L9 orthogonal array design, as shown in Figure 9 and 10. While calculating the S/N ratio for the process capability index of the printed part's diametral deviation, the larger the better option was selected. The objective of minimizing the variation is achieved through setting the goal of closeness of the measured value and designed values.

S/N ratio computation was done by Eq. (5), where n is the total number of trials and  $y_i$  is the observed value of PCI for  $i^{\text{th}}$  trial.

$$S/N_{Cpi} = -10 \log_{10} \left[ \frac{1}{n} \sum_{i=1}^n \frac{1}{y_i^2} \right] \quad (5)$$

Table 3 indicates that parametric setting as per Taguchi's DOE, experiment number 2 indicates the minimum value of diametral deviation 0.166 mm, having corresponding PCI of 2.298 with S/N ratio of 7.227dB.

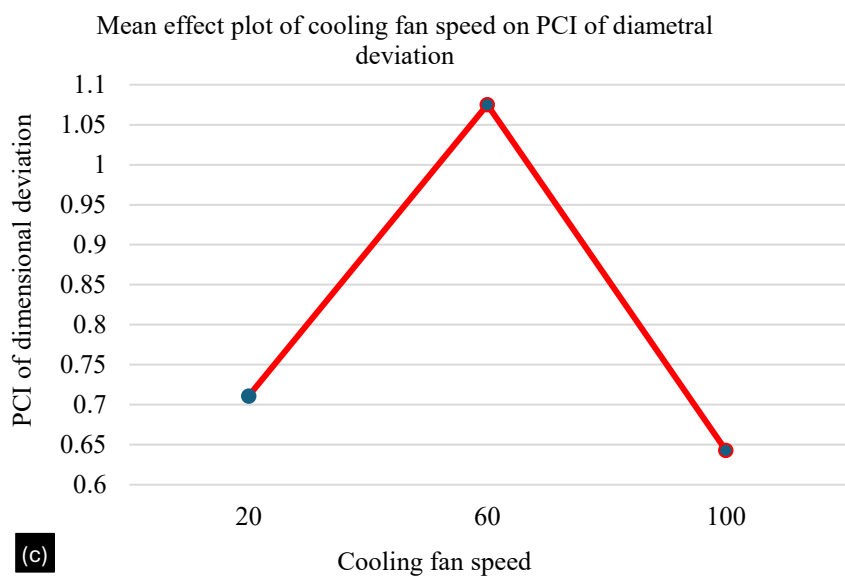
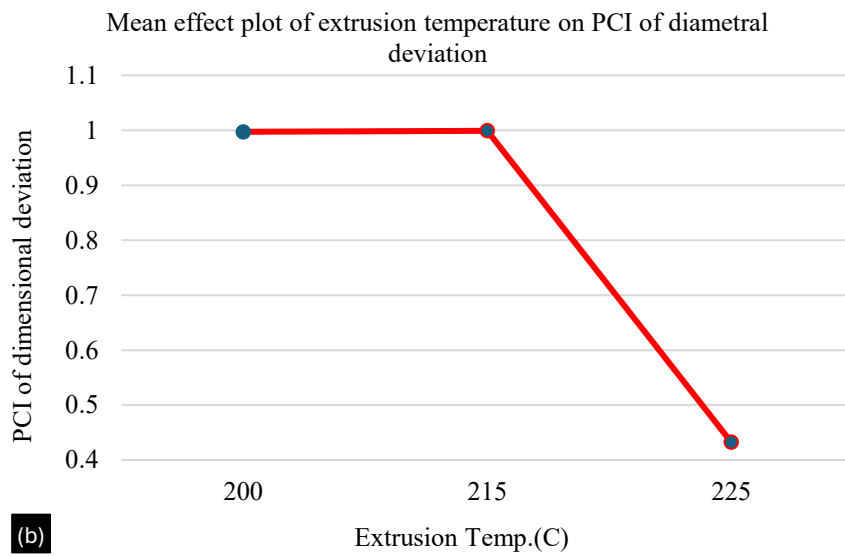
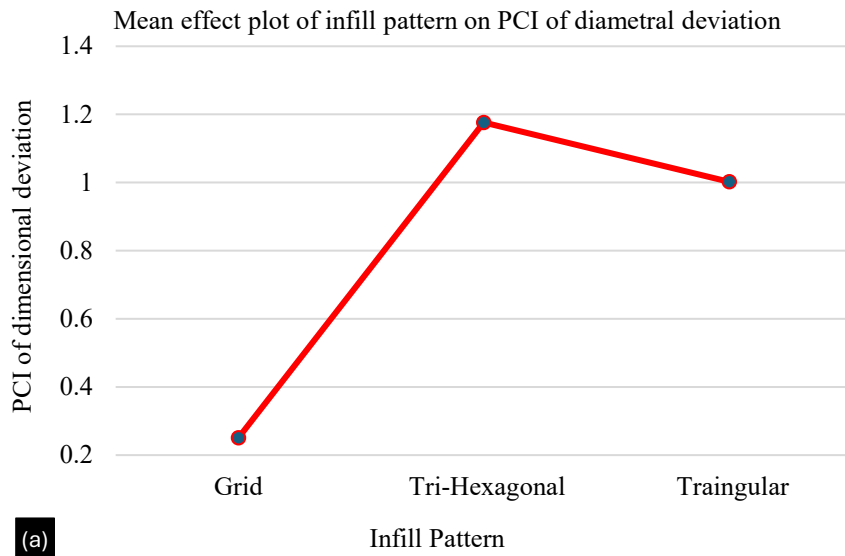
Although some PCI values are below the industrial benchmark of 1.33, the optimal parameter setting identified provides the maximum achievable PCI within the laboratory scale FDM process, offering practical guidance for improving dimensional accuracy.

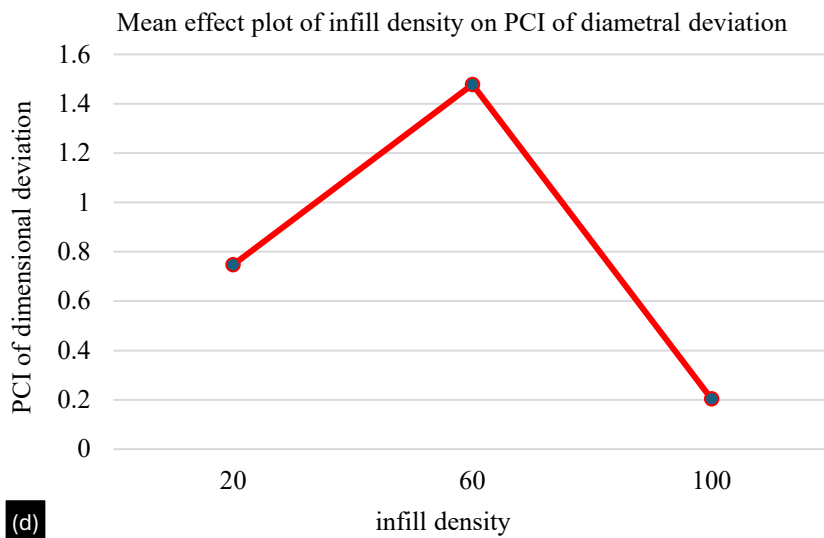
The type of infill pattern was found to be an important parameter among all 3D printing parameters considered for the study. The main effect plot is shown in Figure 9 to describe the behavior of input parameters on PCI of diametral deviation. The optimum parametric combination was selected by higher S/N ratio for PCI for dimensional deviation. The optimal process parametric combination was found to be as follows: Extrusion temperature-200 (°C), Cooling Fan Speed- 60%, Infill Density 60%, and Infill Pattern- Triangular) (Figure 10)

### ANOVA (Analysis of Variance) of PCI of Diametral Deviation:

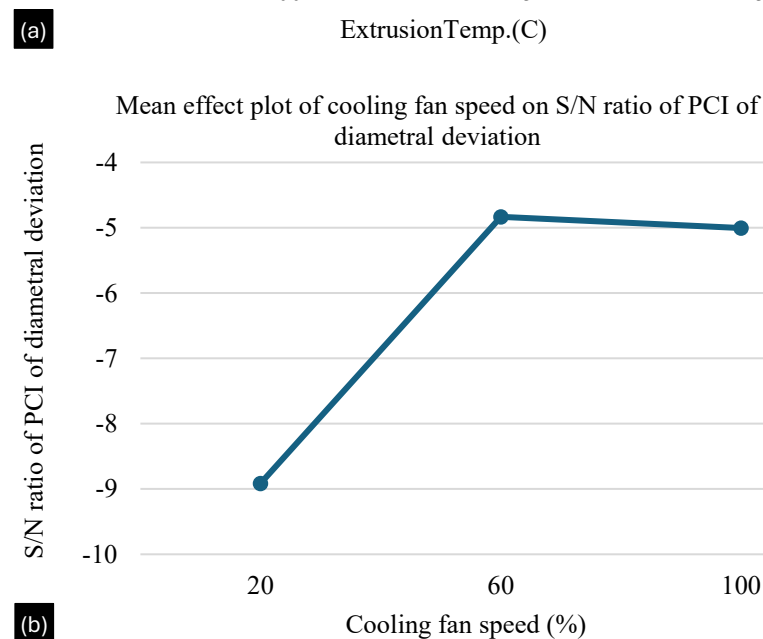
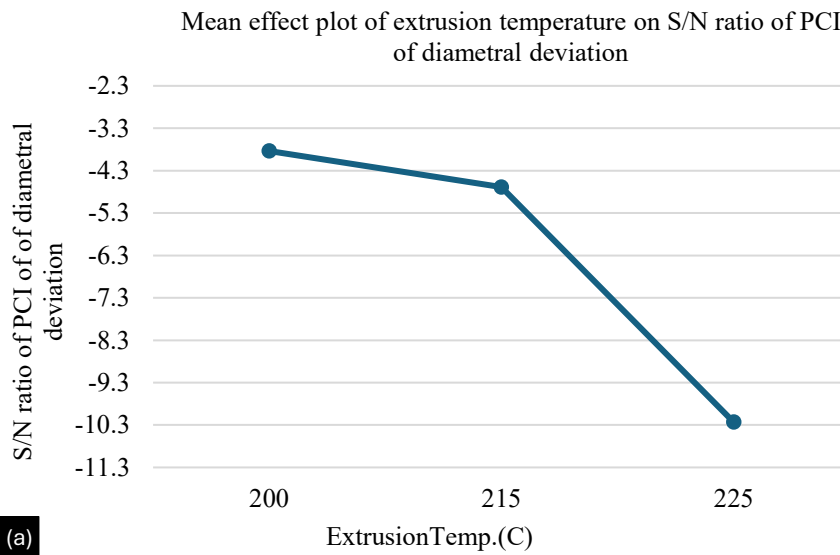
ANOVA was performed on experimental results of values obtained of PCI for diametral deviation. MINITAB software was used to perform the ANOVA on above values.

From Table 5, infill pattern (29.80%) and infill density (9.14%) were found to be influential parameters due to higher F values and percent contribution to affect the PCI values of dimensional deviation of printed specimen.

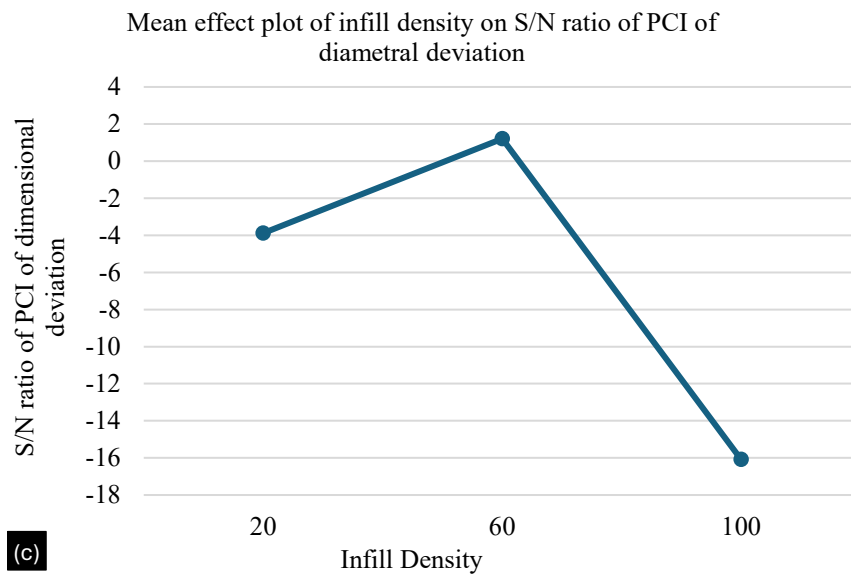




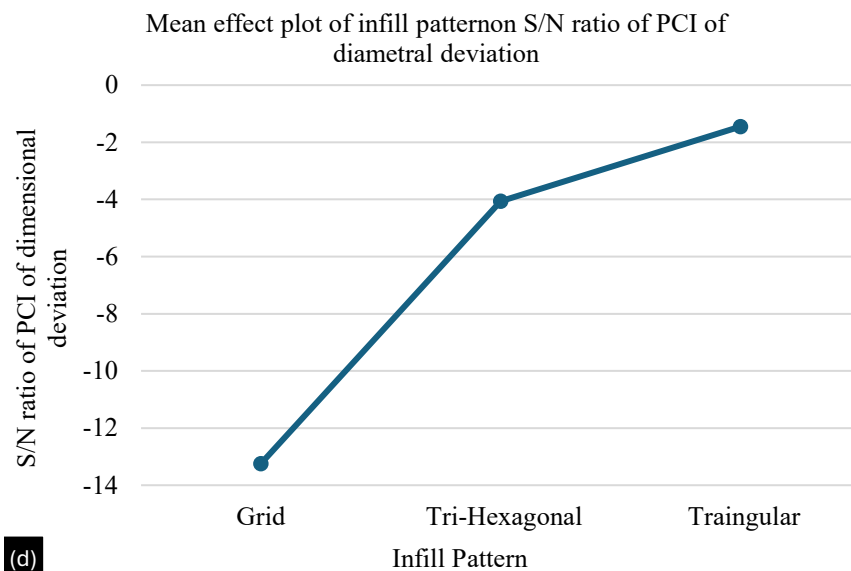
(d) **Figure 9** Mean Effect Plot of Printing Parameters on PCI Of Diametral Deviation



(b)



(c)



(d)

**Figure 10.** Mean Effect Plot of Printing Parameters on S/N Ratio PCI Of Diametral Deviation.

**Table 5.** Analysis Of Variance of S/N Ratio of Diametral Deviation

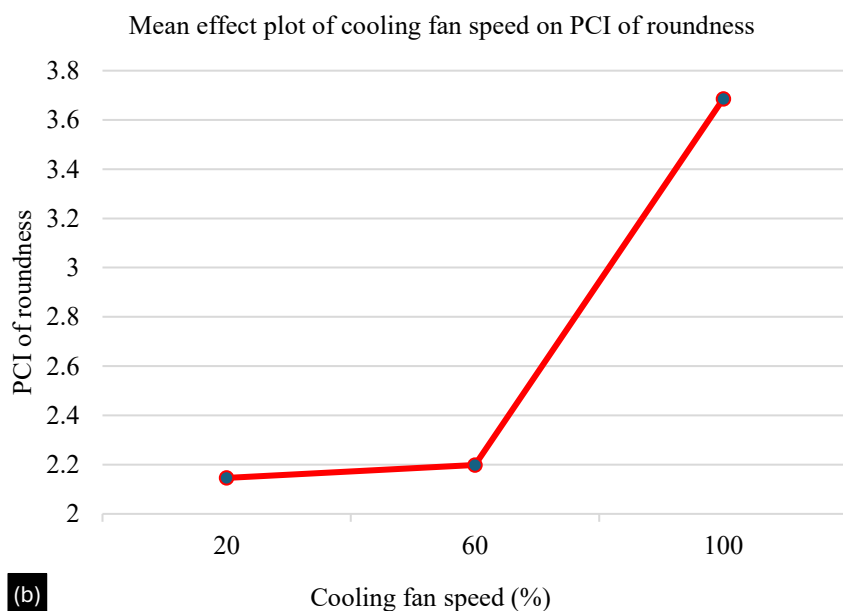
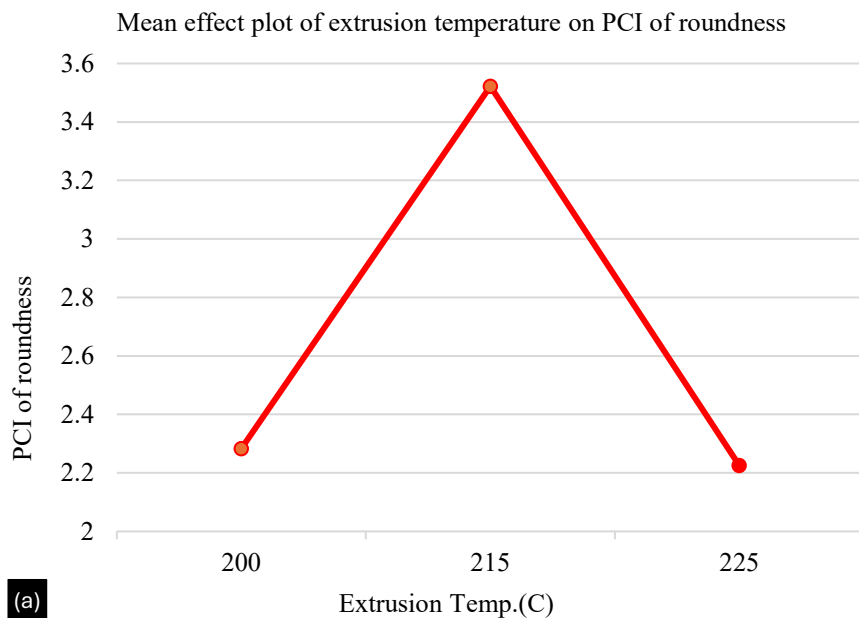
Source	DF	Adj SS	Adj MS	F-Value	% Contribution
Regression	5	2.32	0.46	0.55	--
Extrusion Temperature (°C)	1	0.41	0.41	0.48	8.45
Cooling fan speed (%)	1	0.02	0.02	0.02	0.35
Infill Density (%)	1	0.44	0.44	0.52	<b>9.14</b>
Infill Pattern	2	1.45	0.73	0.85	<b>29.80</b>
Error	3	2.55	0.85		
Total	8	4.87			

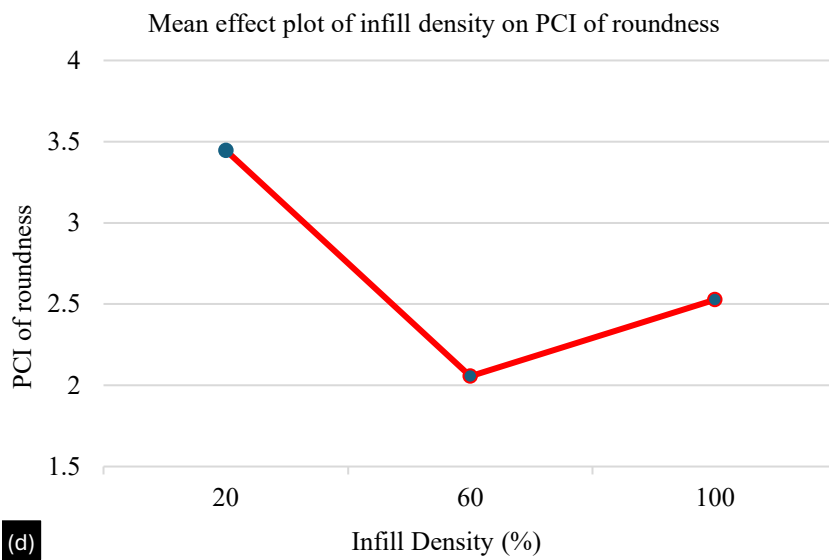
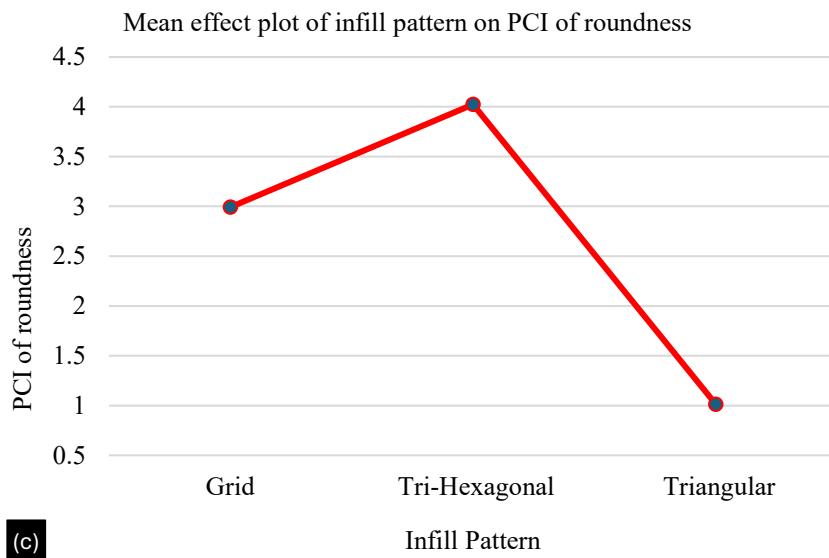
**Roundness**

The degree to which an object's form resembles a complete circle or sphere is referred to as its roundness. It gauges how well an object's outlines deviate the form of a sphere or circle. In many fields

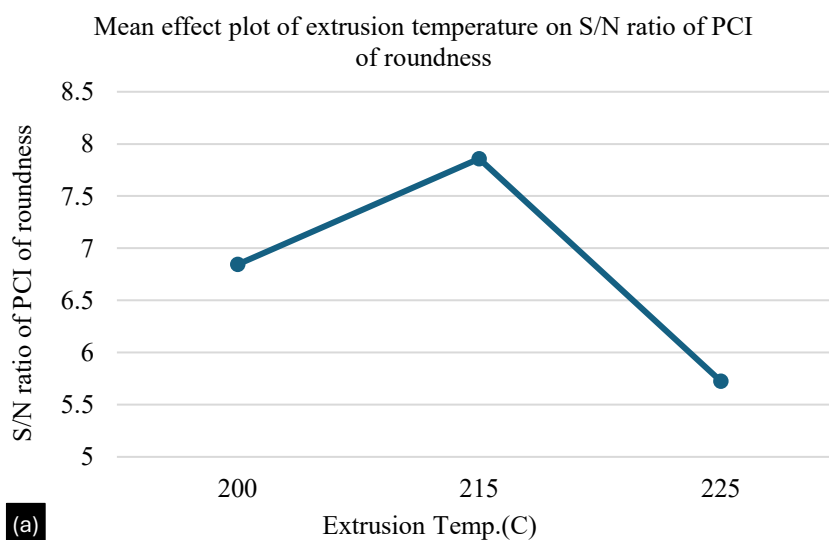
where accuracy is critical, such as manufacturing, metrology, and quality control, roundness is a significant geometric feature.

Similar methodology was adopted as applied for PCI for roundness. The higher the better S/N ratio was selected for maximizing the PCI value of roundness. Table 5 displays the results of PCI for roundness and the S/N ratio. Table 4 indicates that parametric setting as per Taguchi's DOE, experiment number 6 indicates the minimum value of average roundness 0.079 mm, having maximum corresponding PCI of 6.648 with S/N ratio of 16.4538dB. The type of infill pattern was found to be an important parameter among all other parameters for PCI of roundness. The main effect plot is shown in Figure 11 to describe the behavior of input parameters on PCI of roundness. The optimum parametric combination was selected by higher S/N ratio for PCI for roundness. The optimal process parametric combination was found to be as follows: Extrusion temperature-215 (°C), Cooling Fan Speed- 100%, Infill Density 20% and Infill Pattern- Tri-Hexagonal (Figure 12).





**Figure 11.** Mean Effect Plot of Printing Parameters on PCI of Roundness.



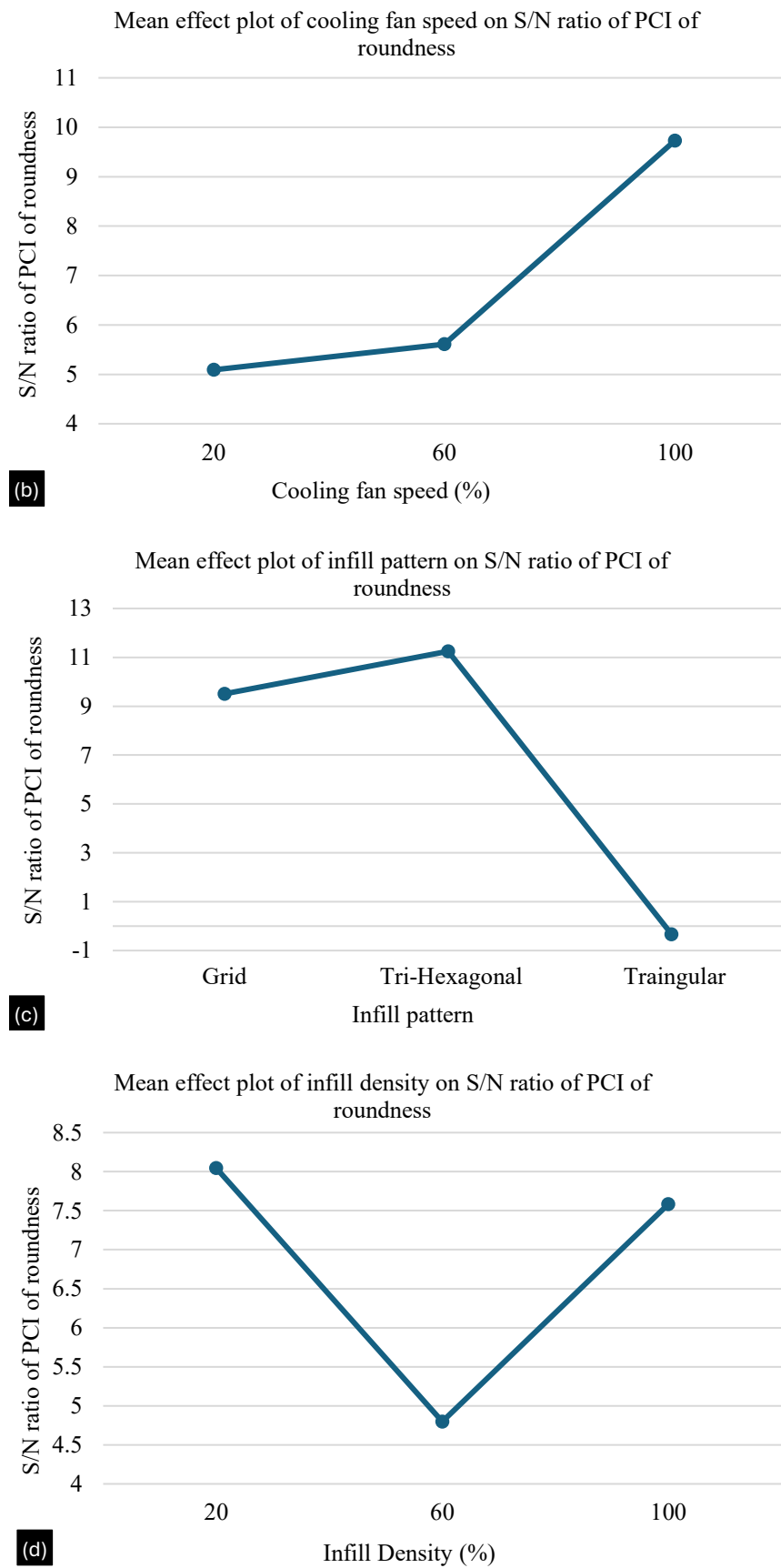


Figure 12. Mean Effect Plot of S/N Ratio of Printing Parameters on PCI of Roundness.

**ANOVA (Analysis of Variance) of PCI of roundness**

ANOVA was performed on experimental results of values obtained of PCI for roundness. It was revealed that infill pattern (Tri-hexagonal shape) is influential parameter (39.25% contribution) to affect the PCI values of roundness of printed specimen. Cooling fan speed was found to be the second important parameter (10.83% contribution) to affect the same printing characteristics (Table 6).

**Table 6.** Analysis of Variance of S/N Ratio of PCI Of Roundness

Source	DF	Adj SS	Adj MS	F-Value	% Contribution
Regression	5	267.787	53.557	5.3	--
Extrusion Temp.(C)	1	1.222	1.222	0.12	0.41
Cooling fan speed (%)	1	32.285	32.285	3.2	<b>10.83</b>
Infill Density (%)	1	0.319	0.319	0.03	0.11
Infill Pattern	2	233.962	116.981	11.58	<b>39.24</b>
Error	3	30.31	10.103		
Total	8	298.097			

The deviation in roundness or diametral deviation value is caused by subsequent deposition of next layer on previously deposited layer. The subsequent printing layer causes deformation if the previous layer is not properly cooled resulting in poor dimensional quality of TPU product. It can be seen from Figure 10 and 12 that cooling fan speed at 60% and 1000% is suitable for achieving good diametral deviation and roundness.

It can be inferred from the results that cooling fan speed should not be set at lower value for printing of TPU material.

It is evident from the results that infill density should not be set at higher values (100%). It can be set at lower value (20%) or mid-level (60%) to achieve higher accuracy in roundness and dimensional deviation respectively in TPU printing. It can be attributed to the fact that 100% infill density causes the low porosity of parts. Low porous material does not accommodate the any extra molten material coming out of the nozzle (oozing effect). This causes printing of the swelled parts in TPU printing. On the contrary, the lower density causes the high porosity of printed part accommodating the extra molten material coming out from the nozzle. This results in higher accuracy of printed parts.

It may be inferred from the results that lower to medium infill densities yields optimal PCI for diametral deviation and roundness. The lower to medium infill densities develops the thermal balance which minimizes the warping and distortion ensuring adequate interlayer bonding with improved dimensional accuracy.

Among all the infill patterns utilized in 3D printing, including the grid and triangle infill kinds, the tri-hexagonal shape is the strongest. Triangles are scattered across a hexagonal pattern created by this pattern crossing over itself.

The triangular pattern places plastic in a triangular grid that crosses over to 60°C, whereas plastic is laid down using a grid pattern that resembles a cubic and crosses over itself at right angles. Tri hexagon and triangular pattern can be referred to achieve high accuracy in terms of roundness and dimensional deviation respectively, as both types of patterns reduce the possibility of distortion and warping during printing as compared to grid patterns.

**Confirmation Experiment**

The confirmatory experiment was conducted to validate the results of PCI obtained under optimized parametric conditions. The predicted PCI was calculated by the following formula.

$$\begin{aligned} \mu &= \bar{T} + (\bar{X}_2 - \bar{T}) + (\bar{Y}_2 - \bar{T}) \\ &= \bar{X}_2 + \bar{Y}_2 - \bar{T} \end{aligned} \tag{6}$$

Where  $\bar{T}$  = Overall mean of the response

$\bar{X}_2, \bar{Y}_2$  = Average values of response at the optimized levels of parameters

The predicted PCI and PCI obtained from confirmatory experiments were found to be close to each other exhibiting close correlation. A remarkable improvement of PCI is shown in Table 7 justifying the experimental results.

**Table 7.** Confirmatory Results

Experimental condition	Roundness	PCI	Diametral Deviation	PCI
Process parametric condition	Extrusion Temperature (200°C), Cooling fan speed (20%), Infill Density (20%), Infill Pattern (Grid)	2.839	Extrusion Temperature (200°C), Cooling fan speed (20%), Infill Density (20%), Infill Pattern (Grid)	0.278
Predicted Value	Extrusion Temperature (215°C), Cooling fan speed (100%), Infill Density (20%), Infill Pattern (Tri-hexagonal)	6.648	Extrusion Temperature (200°C), Cooling fan speed (60%), Infill Density (60%), Infill Pattern (Triangular)	2.123
Experimental Value	Extrusion Temperature (215°C), Cooling fan speed (100%), Infill Density (20%), Infill Pattern (Tri-hexagonal)	6.695	Extrusion Temperature (200°C), Cooling fan speed (60%), Infill Density (60%), Infill Pattern (Triangular)	2.198

## CONCLUSION

The goal of this study is to use the Taguchi approach to identify the best parametric setting for the 3D printing process in order to reduce the process capability index. Extrusion temperature (200°C), cooling fan speed (60%) the infill density (60%) and the infill pattern (triangular) for precise diametral deviation were determined to be the best process parameters for 3D printing based on the studies that were done. The combination of optimum process parameters produces process capability index for diametral deviation and S/N ratio values as 2.298 and 7.227 dB respectively. Based on ANOVA analysis infill pattern (29.80%) and infill density (9.14%) were found to be significant process parameters for PCI of diametral deviation.

The optimum process parametric condition for accurate roundness was found to be extrusion temperature (215°C), cooling fan speed (100%), infill Density (20%) and infill Pattern (Tri-hexagonal). The combination of optimum process parameters produces process capability index for roundness and S/N ratio values 6.648 and 16.453 dB respectively. Based on ANOVA analysis infill pattern (39.25%) and cooling fan speed (10.83%) were found to be significant process parameters for PCI of roundness.

While this study has focused on improving the process capability of TPU components fabricated through FDM, more work can be done in this area. Upcoming studies may investigate the role of other factors such as variations in nozzle temperature, part cooling techniques, and alternative printing paths to further enhance accuracy and strength.

Incorporating intelligent systems like machine learning and in-process monitoring could help in adjusting settings automatically for better quality. Research can also be extended to new material blends, composite filaments, or graded structures to widen the applications of TPU parts in flexible products, healthcare, and wearables. Finally, testing how these optimized parts perform over longer

periods and in real working conditions would help in making FDM TPU parts more suitable for industry use.

### CONFLICTS OF INTEREST

There is no conflict of interest.

### FUNDING

This paper has received no external funding.

### REFERENCES

1. Mohamed OA, Masood SH, Bhowmik JL. Optimization of fused deposition modeling process parameters: a review of current research and future prospects. **Adv Manuf.** 2015;3(1):42–53. doi:10.1007/s40436-014-0097-7.
2. Sood AK, Ohdar RK, Mahapatra SS. Parametric appraisal of mechanical property of fused deposition modelling processed parts. **Mater Des.** 2010;31(1):287–295. doi:10.1016/j.matdes.2009.06.016.
3. Chohan JS, Singh R, Boparai KS, Penna R, Fraternali F. Dimensional accuracy analysis of coupled fused deposition modeling and vapour smoothing operations for biomedical applications. **Compos B Eng.** 2017;117:138–149. doi:10.1016/j.compositesb.2017.02.045.
4. Dey A, Yodo N. A systematic survey of FDM process parameter optimization and their influence on part characteristics. **J Manuf Mater Process.** 2019;3(3):64. doi:10.3390/jmmp3030064.
5. Williams JM, Adewunmi A, Schek RM, et al. Bone tissue engineering using polycaprolactone scaffolds fabricated via selective laser sintering. **Biomaterials.** 2005;26(23):4817–4827. doi:10.1016/j.biomaterials.2004.11.057.
6. Exconde MKJE, Co JAA, Manapat JZ, Magdaluyo ER. Materials selection of 3D printing filament and utilization of recycled polyethylene terephthalate (PET) in a redesigned breadboard. **Procedia CIRP.** 2019;84:28–32. doi:10.1016/j.procir.2019.04.337.
7. Bates SRG, Farrow IR, Trask RS. 3D printed polyurethane honeycombs for repeated tailored energy absorption. **Mater Des.** 2016;112:172–183. doi:10.1016/j.matdes.2016.08.062.
8. Hu B, Li M, Jiang J, Zhai W. Development of microcellular thermoplastic polyurethane honeycombs with tailored elasticity and energy absorption via CO<sub>2</sub> foaming. **Int J Mech Sci.** 2021;197:106324. doi:10.1016/j.ijmecsci.2021.106324.
9. Qi HJ, Boyce MC. Stress–strain behavior of thermoplastic polyurethanes. **Mech Mater.** 2005;37(8):817–839. doi:10.1016/j.mechmat.2004.08.001.
10. Chen Q, Mangadlao JD, Wallat J, De Leon A, Pokorski JK, Advincula RC. 3D printing biocompatible polyurethane/poly(lactic acid)/graphene oxide nanocomposites: anisotropic properties. **ACS Appl Mater Interfaces.** 2017;9(4):4015–4023. doi:10.1021/acsami.6b11793.
11. Kang KS, Jee C, Bae JH, Jung HJ, Huh P. Heat capacity variables of thermoplastic polyurethane for high-quality 3D printing resolution and their characteristics. **Mater Lett.** 2019;257:126698. doi:10.1016/j.matlet.2019.126698.
12. Garg N, Rastogi V, Kumar P. Process parameter optimization on the dimensional accuracy of additive manufacture thermoplastic polyurethane (TPU) using RSM. **Mater Today Proc.** 2022. doi:10.1016/j.matpr.2022.02.309.
13. Dixit N, Jain PK. Effect of fused filament fabrication process parameters on compressive strength of thermoplastic polyurethane and polylactic acid lattice structures. **J Mater Eng Perform.** 2022;31:5973–5982. doi:10.1007/s11665-022-06664-0.
14. Rattanapan S, Pasetto P, Pilard J, Tanrattanakul V. Polyurethane foams from oligomers derived from waste tire crumbs and polycaprolactone diols. **J Appl Polym Sci.** 2016;133(47):44251. doi:10.1002/app.44251.
15. Tseng HH, Lin ZY, Chen SH, Lai WH, Wey MY. Reuse of reclaimed tire rubber for gas-separation membranes prepared by hot-pressing. **J Clean Prod.** 2019;237:117739. doi:10.1016/j.jclepro.2019.117739.

16. Lin TA, Lin JH, Bao L. Polypropylene/thermoplastic polyurethane blends: mechanical characterizations, recyclability and sustainable development of thermoplastic materials. **J Mater Res Technol.** 2020;9(3):5304–5312. doi:10.1016/j.jmrt.2020.03.056.
17. Lin TA, Lin JH, Bao L. A study of reusability assessment and thermal behaviors for thermoplastic composite materials after melting process: polypropylene/thermoplastic polyurethane blends. **J Clean Prod.** 2021;279:123473. doi:10.1016/j.jclepro.2020.123473.
18. Lee CS, Kim SG, Kim HJ, Ahn SH. Measurement of anisotropic compressive strength of rapid prototyping parts. **J Mater Process Technol.** 2007;187–188:627–630. doi:10.1016/j.jmatprotec.2006.11.095.
19. Pandey PM, Reddy V, Dhande SG. Improvement of surface finish by staircase machining in fused deposition modeling. **J Mater Process Technol.** 2003;132:323–331. doi:10.1016/S0924-0136(02)00953-6.
20. Dhande SG. Slicing procedures in layered manufacturing: a review. **Rapid Prototyp J.** 2003;9:274–288. doi:10.1108/13552540310502185.
21. Ahn SH, Montero M, Odell D, Roundy S, Wright PK. Critical parameters influencing the quality of prototypes in fused deposition modelling. **J Mater Process Technol.** 2001;118:385–388. doi:10.1016/S0924-0136(01)00980-3.
22. Tanoto YY, Anggono J, Siahaan IH, Budiman W. The effect of orientation difference in fused deposition modeling of ABS polymer on the processing time, dimension accuracy, and strength. **AIP Conf Proc.** 2017:030051. doi:10.1063/1.4968304.
23. Chohan JS, Singh R. Enhancing dimensional accuracy of FDM based biomedical implant replicas by statistically controlled vapor smoothing process. **Prog Addit Manuf.** 2016;1(1–2):105–113. doi:10.1007/s40964-016-0009-4.
24. Sahu RK, Mahapatra SS, Sood AK. A study on dimensional accuracy of fused deposition modeling (FDM) processed parts using fuzzy logic. **J Manuf Sci Prod.** 2013;13(3):183–197. doi:10.1515/jmsp-2013-0010.
25. Padhi SK, Panda BN, Satpathy MP, et al. Optimization of fused deposition modeling process parameters using a fuzzy inference system coupled with Taguchi philosophy. **Adv Manuf.** 2017;5(3):231–242. doi:10.1007/s40436-017-0187-4.
26. Akande SO. Dimensional accuracy and surface finish optimization of fused deposition modelling parts using desirability function analysis. **Int J Eng Res Technol.** 2015;4(4):1–8.
27. Kumar M, Rajiyan J, Gupta P. A computational approach for solving elasto-statics problems. **Mater Today Proc.** 2021;46(15):6876–6879. doi:10.1016/j.matpr.2021.04.462.
28. Pasupuleti T, Natarajan M, Naik RM, Silambarasan R. Optimization of fused deposition modeling using Taguchi-based grey relational analysis for TPU used in auto parts. **SAE Tech Pap.** 2025;28-0158. doi:10.4271/2025-28-0158.
29. Pasupuleti T, Natarajan M, D P, A G. Development of ANFIS predictive model for additive manufacturing of TPU material. **SAE Tech Pap.** 2024;28-0025. doi:10.4271/2024-28-0025.
30. Xavier G, Marino K, Yannick N, Efe CB, Alisa R, John L. Data-driven process optimization of fused filament fabrication based on in situ measurements. **IFAC Pap Online.** 2023;56(2):4713–4718.
31. Jingyi W, Panayiotis P. Finite element analysis-enabled optimization of process parameters in additive manufacturing. **Finite Elem Anal Des.** 2025;244:104282.
32. Yadavalli V, Myadam A, Telu S. FDM 3D-print on thermoplastic polyurethane (TPU) with different process parameters using gyroid and zigzag infill patterns. **Open Access Libr J.** 2024;11:1–15. doi:10.4236/oalib.1111203.
33. Portoacă AI, Ripeanu RG, Diniță A, Tănase M. Optimization of 3D printing parameters for enhanced surface quality and wear resistance. **Polymers.** 2023;15(16):3419. doi:10.3390/polym15163419.